Molecular Biology of the Cell
Vol. 21, 3680–3692, November 1, 2010

Dynamics of Multiple Nuclei in *Ashbya gossypii* Hyphae Depend on the Control of Cytoplasmic Microtubules Length by Bik1, Kip2, Kip3, and Not on a Capture/Shrinkage Mechanism

Sandrine Grava and Peter Philippsen

Department of Molecular Microbiology, Biozentrum, University of Basel, CH-4056 Basel, Switzerland

Submitted June 21, 2010; Revised August 19, 2010; Accepted September 2, 2010
Monitoring Editor: Kerry S. Bloom

***Ashbya gossypii* has a budding yeast-like genome but grows exclusively as multinucleated hyphae. In contrast to budding yeast where positioning of nuclei at the bud neck is a major function of cytoplasmic microtubules (cMTs), *A. gossypii* nuclei are constantly in motion and positioning is not an issue. To investigate the role of cMTs in nuclear oscillation and bypassing, we constructed mutants potentially affecting cMT lengths. Hyphae lacking the plus (+)end marker Bik1 or the kinesin Kip2 cannot polymerize long cMTs and lose wild-type nuclear movements. Interestingly, hyphae lacking the kinesin Kip3 display longer cMTs concomitant with increased nuclear oscillation and bypassing. Polymerization and depolymerization rates of cMTs are 3 times higher in *A. gossypii* than in budding yeast and cMT catastrophes are rare. Growing cMTs slide along the hyphal cortex and exert pulling forces on nuclei. Surprisingly, a capture/shrinkage mechanism seems to be absent in *A. gossypii*. cMTs reaching a hyphal tip do not shrink, and cMT +ends accumulate in hyphal tips. Thus, differences in cMT dynamics and length control between budding yeast and *A. gossypii* are key elements in the adaptation of the cMT cytoskeleton to much longer cells and much higher degrees of nuclear mobilities.**

INTRODUCTION

Cytoplasmic microtubules (cMTs) have been shown to play an essential role in nuclear movement and positioning in many organisms, i.e., during yeast cell division, embryo development in *Caenorhabditis elegans*, and *Drosophila melanogaster* neuron development (Ahringer, 2003). Two important features are required for cMTs to control nuclear movement and positioning: 1) their high dynamicity and 2) their ability to interact with the cell cortex. cMTs are intrinsically polar polymers with a slow-growing minus (−)end associated with the microtubule organizing center (MTOC) and a fast-growing plus (+)end (also called +tip) oriented peripherically (Desai and Mitchison, 1997; Carvalho *et al*., 2003). The cMT +ends are highly dynamic structures that undergo phases of polymerization and depolymerization, leading to frequent collisions with the cell cortex. The overall length of a cMT depends on the balance of growth, shrinkage, and pause phases termed dynamic instability. This balance seems to be mainly controlled by kinesin motor proteins and +end-tracking proteins (+TIPS).

This article was published online ahead of print in *MBoC in Press* (http://www.molbiolcell.org/cgi/doi/10.1091/mbc.E10–06–0527) on September 15, 2010.

Address correspondence to: Peter Philippsen (peter.philippsen@unibas.ch).

Abbreviations used: cMT, cytoplasmic microtubule; SPB, spindle pole body.

Fungal and metazoan members of the kinesin-8, kinesin-13, and kinesin-14 family have been shown to directly regulate cMT dynamics by promoting their depolymerization (Moore and Wordeman, 2004; Sproul *et al*., 2005; Gupta *et al*., 2006; Varga *et al*., 2006). The +TIPS specifically associate with the +end of cMTs (Galjart and Perez, 2003). Many of them have important roles in controlling +end dynamics by promoting cMT stability (Brunner and Nurse, 2000; Komarova *et al*., 2002). The mammalian +TIP protein CLIP-170 and its budding yeast orthologue Bik1 are also crucial for cMT interactions with the cell cortex and for targeting of dynein at cMT +ends (Coquelle *et al*., 2002; Sheeman *et al*., 2003; Carvalho *et al*., 2004).The +tip localization of Bik1 seems to depend on the kinesin Kip2 (Carvalho *et al*., 2004).

In budding yeast, nuclear movements have been described to be random or directed (DeZwaan *et al*., 1997; Shaw *et al*., 1997; Lee *et al*., 1999; Adames *et al*., 2000). In G1 phase, nuclei are randomly pushed in all directions by the growth of cMTs against the cortex. Then, after spindle pole body (SPB) duplication and bud emergence, nuclear movements become directed. cMTs that have been captured by the bud neck or the bud tip shrink to move the nucleus close to the bud neck (capture/shrinkage step). This requires a high dynamicity of cMTs (DeZwaan *et al*., 1997; Shaw *et al*., 1997; Lee *et al*., 1999; Kusch *et al*., 2002). In early anaphase, the dynein pathway triggers the sliding of cMTs along the bud cortex to pull the nucleus through the narrow bud neck (Adames and Cooper, 2000).

The filamentous fungus *Ashbya gossypii* is an interesting model to study the evolution of the cMT cytoskeleton and nuclear migration because its genome is closely related to the budding yeast genome (Dietrich *et al*., 2004), but their cMT cytoskeleton and nuclear mobility are markedly different. In contrast to budding yeast, *A. gossypii* grows as very

long nondividing multinucleated hyphae and a particular positioning of nuclei even during mitosis is not required. Nuclear migration in *A. gossypii* consists of frequent and independent oscillations (short-range back-and-forth movements) and bypassings (1 nucleus overtakes 1 or a few nuclei) with a net nuclear movement of nuclei toward the growing hyphal tips (Alberti-Segui *et al*., 2001; Gladfelter and Berman, 2009; Lang *et al*., 2010a,b).

SPBs are the only MTOCs in *A. gossypii*. They are embedded in the nuclear envelope and can nucleate up to six cMTs of variable length and variable orientation at their outer plaques (Lang *et al*., 2010a). *A. gossypii* cMTs are up to 10 times longer than budding yeast cMTs (Tirnauer *et al*., 1999; Lang *et al*., 2010a). Using microtubule (MT)-destabilizing drugs, it has been shown that the overall forward movement of nuclei does not required cMTs but is rather a cotransport of nuclei with the cytoplasmic stream, whereas nuclear oscillation and bypassing are cMT-dependent processes (Alberti-Segui *et al*., 2001; Lang *et al*., 2010a,b). However, what exactly generates those nuclear movements is still poorly understood. It has been hypothesized that intrinsic dynamics of cMTs and/or MT-motor proteins could be responsible for them.

Because orthologues of all proteins involved in cMT dynamics and the control of nuclear migration in budding yeast are conserved in *A. gossypii*, we were wondering why can cMTs grow so long in *A. gossypii*. Hyphae of *A. gossypii* are much longer than budding yeast cells, and one could argue that cMT length had to adapt to hyphal length to transport vesicles to the growing tips. However, this hypothesis can be excluded because, like in budding yeast, and in contrast to other filamentous fungi or mammalian cells, cMTs are not required for cell growth in *A. gossypii* (Alberti-Segui *et al*., 2001; Wendland and Walther, 2005; Kohli *et al*., 2008).

To understand the cellular role of long cMTs in *A. gossypii*, we asked how does the control of cMT length influence nuclear oscillation and bypassing events. We investigated the MT polymerization and depolymerization rates and frequencies of cMTs and studied the role of the +tip MT binding protein Bik1 and the kinesins Kip2 (Kinesin-7) and Kip3 (Kinesin-8) in cMT dynamics. We then asked whether cMTs interact with specific cortical sites and how cMTs interact with the cell cortex to induce nuclear movements. Are nuclear movements triggered by cMT pushing, pulling, sliding, or shrinking forces? The results we present here contribute to the understanding of how A. *gossypii* and budding yeast, with basically the same components, adapted nuclear migration to specific cellular needs.

MATERIALS AND METHODS

A. gossypii Media and Growth Conditions

A. gossypii media and culturing protocols are described in Ayad-Durieux *et al.* (2000) and Wendland *et al.* (2000). Strains were grown in *Ashbya* full medium (AFM medium: 1% bactopeptone, 1% yeast extract, 2% glucose, and 0.1% *myo*-inositol) at 30°C. Transformants derived from *A. gossypii* reference strains were selected on AFM plates containing 200 mg/ml G418 (geneticin; ForMedium Ltd., Hunstanton, Norfolk, England) or 50 μg/ml ClonNAT (Werner BioAgents, Jena, Germany). To test the effect of benomyl on growth, AFM plates were prepared by adding 33–132 μM benomyl (Sigma-Aldrich, St. Louis, MO; dissolved in dimethyl sulfoxide [DMSO]) directly into the medium before pouring the plates.

Strain Construction

A. gossypii transformation protocols are described in Ayad-Durieux *et al.* (2000) and Wendland *et al.* (2000). All strains constructed in this study were derived from reference strains expressing either a histone H4-green fluorescent protein (GFP) fusion (ASG46 strain: ADE2-HHF1-yeGFP; Gladfelter *et al*., 2006) or an exogenous GFP-tubulin1 fusion (ADE2-GFP-AgTUB1; Lang *et al*., 2010a). *A. gossypii* deletion mutants were made by a polymerase chain reaction (PCR)-based one-step gene-targeting approach (Wendland *et al*., 2000). PCR were performed using standard methods with *Taq* polymerase from Roche Diagnostics (Mannheim, Germany), and oligonucleotides were synthesized at Microsynth (Balgach, Switzerland). Oligonucleotide primers are listed in Supplemental Table S1.

For gene deletions, *A. gossypii* cells were transformed with PCR products amplified with the pAG140 (GEN3) or pAG100 (NAT) templates and the "gene name"-del5/del3 oligonucleotide pairs, which contained 45-base pair homology upstream and downstream of the open reading frames. The primary transformation produces heterokaryon cells, which have a mixture of "wild-type" (WT) and transformed nuclei. Transformed heterokaryons were verified with oligonucleotide pairs gene name-VER5/G2.2 and gene name-VER3/G3.3 for GEN3 cassettes (gene name-VER5/V2*NAT1 and gene name-VER3/V3*NAT1 for NAT cassettes; Supplemental Table 1). Three homokaryons (obtained after sporulation of 3 independent verified transformants) were characterized for each mutant.

For the Bik1-Cherry fusion, a Cherry-NAT-tagging cassette was generated by PCR using as a template the pAGT211 plasmid (Kaufmann, 2009) and the primers BIK1-DEL3 and BIK1-TAG (homologous to the 45 base pairs upstream of the Ag*BIK1* stop codon). The resulting PCR product was directly transformed into GFP-Tub1 *A. gossypii* cells. Verifications of the heterokaryons and homokaryons were performed as described above with the primer pairs BIK1-VER3/V3*NAT1.

Immunofluorescence and Time-Lapse Microscopy

The microscope used was an Axioplan 2 imaging microscope equipped with the objectives Plan-Apochromat 100 × 1.40-numerical aperture oil differential interference contrast (DIC) and Plan-Apochromat 63 × 1.40-numerical aperture oil DIC (Carl Zeiss, Feldbach, Switzerland) and appropriate filters (Carl Zeiss and Chroma Technology, Brattleboro, VT). The light source for fluorescence microscopy was a Polychrome V monochromator (TILL Photonics, Gräfelfing, Germany). Images were acquired at room temperature using a CoolSNAP HQ cooled charge-coupled device camera (Photometrics, Tucson, AZ) with MetaMorph 6.2r6 software (Molecular Devices, Sunnyvale, CA). The distance between two planes in stack acquisitions was set to 1 μm for H4-GFP movies and to 0.3 μm for anti-tubulin stainings. Brightness and contrast were adjusted using MetaMorph's "scale image" command. Stacks were deconvolved with MetaMorph's "2-D deconvolution" module and flattened by maximum projection with the "stack arithmetic" function. The Bik1-Cherry GFP-Tub1 movies were 1Z plane movies treated with Flatten Background/Kernel/Equalize light functions. Images were colored and overlaid using MetaMorph's "overlay images" command. Time-lapse picture series were processed as described above and converted into QuickTime MPEG-4 movies (QuickTime Player Pro; Apple Computer, Cupertino, CA). Immunofluorescence stainings were performed as described previously (Ayad-Durieux *et al*., 2000; Gladfelter *et al*., 2006). Rat anti-α-tubulin (YOL1/34; Serotec, Oxford, United Kingdom) was used at a 1:50 dilution and Alexa Fluor 568 goat anti-rat immunoglobulin G (Invitrogen, Carlsbad, CA) at a 1:200 dilution. For time-lapse acquisition, small pieces of 2-d-old mycelium were cultured on agarose slides as described previously (Lang *et al*., 2010a).

RESULTS

While Growing, A. gossypii cMTs Accumulate Bik1 at Their +End

It has been shown recently that cMTs in *A. gossypii* are all nucleated from SPB embedded in the nuclear envelope and that SPBs can nucleate up to six cMTs. Short cMTs (<5 μm) spread from SPBs in all directions and long cMTs (up to 25 μm) align along the polarity axis in the direction of the hyphal tip, or opposite to it (Lang *et al*., 2010a). Due to the high complexity of cMT organization in multinucleated hyphae, the low fluorescence of GFP-labeled MTs and the need to restrict movies to 1Z plane for a better time resolution, it has been so far difficult to carefully measure cMT dynamics in *A. gossypii*. cMTs apparently pausing or shrinking could actually grow or slide in another focal planes. In budding yeast, the Bik1 protein associates with +ends of growing, shrinking, and pausing cMTs (Carvalho *et al*., 2004). We therefore investigated cMT dynamics in *A. gossypii* by using time-lapse microscopy with cells expressing GFP-Tub1 (α-tubulin) from an extra gene copy and Bik1-Cherry from the endogenous gene locus. This strain was fully functional because it grew with the same rate that the GFP-Tub1 strain and did not display the characteristic bik1Δ phenotype (see below). The amino acid sequence of AgBik1 (497 aa) shares 37.0% identity with the Bik1 protein (440 aa) of budding yeast. The N-terminal CAP-Gly MT-binding domain of

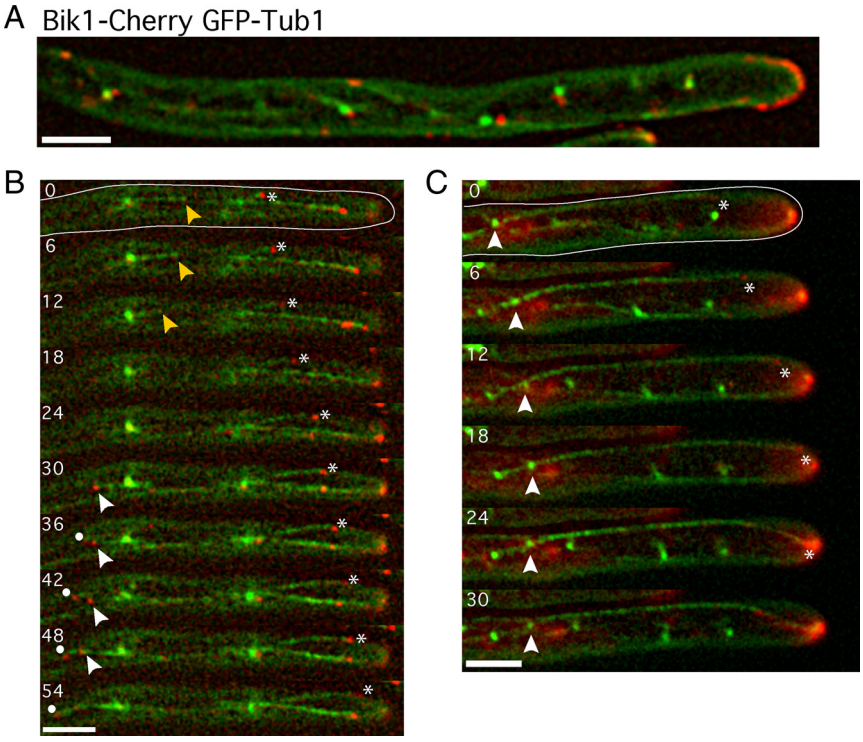

Figure 1. Bik1 protein localizes at +tips of growing cMTs. (A) 1Z plane picture has been taken in the middle of an ~50-μm-long hypha expressing Bik1-Cherry (red) GFP-Tub1(green). (B) White symbols show Bik1 dots at the tip of growing cMTs. The yellow arrowhead points out an apparently shrinking cMT. (C) A very long cMT reaches the hyphal tip. Asterisk (*) and arrowheads track the cMT +tip and the SPB, respectively. Time is indicated in seconds. Bars, 5 μm.

AgBik1 (aa 1-81) shares 70.4% identity with ScBik1. The Bik1-Cherry signal was observed throughout the length of hyphae, especially at cortical sites, adjacent to SPBs and at hyphal tips (Figure 1A). As suggested in budding yeast, the colocalization of Bik1 with SPBs could be either due to Bik1 binding to the kinetochore or to the +end of very short cMTs (Lin *et al*., 2001). As shown in Figure 1B, AgBik1 also could be observed as bright dots at cMT +ends. Those dots, in continuous motion and frequently moving along the cell cortex, clearly colocalized with the +tip of GFP-labeled MTs (Figure 1, B and C). +ends can be >25 μm distant from −ends and long cMTs can overtake several SPBs or nuclei to finally reach the hyphal tip (Figure 1C).

A. gossypii cMTs Grow Faster and Shrink Less Frequently than Saccharomyces cerevisiae cMTs

In budding yeast, cMT growth phases and shrinkage phases can both last for more than a minute with a catastrophe frequency of 2.16 events/min and a rescue frequency of 1.80 events/min (Adames *et al*., 2001). To measure MT dynamics in *A. gossypii*, we tracked 18 cMTs showing a Bik1 signal at their +tip for 0.5–2.5 min. They were followed until the green and red fluorescent signals at their +ends became faint and fuzzy, suggesting that they were moving in another focal plane. Interestingly, those 18 cMTs were in constant growing phase and did not show any dynamic instability. One cMT steadily grew 13.2 μm in 168 s. The small variations in MT length observed in Figure 2A probably resulted from measurement mistakes due to slight movements of the SPB and cMTs out of the focal plane. Three consecutives frames of cMT shrinkage were never observed during the 213 time frames of cMT measurements. For those 18 cMTs, we calculated that the cMT polymerization rate was 0.108 ± 0.035μm/s (mean ± SD; n = 18; Figure 2A). Interestingly, this rate is 3 times higher than the rate of budding yeast (*A. gossypii*, 6.5 μm/min vs. *S. cerevisiae*, 2.2 μm/min; Tirnauer *et al*., 1999; Adames *et al*., 2001; Caudron *et al*., 2008). This increased cMT polymerization rate could partly explain why cMTs are overall longer in *A. gossypii* compared with budding yeast.

In our whole GFP-Tub1 Bik1-Cherry movie collection (>100 cMTs), we could only observe a very low number of shrinking cMTs (n = 6). In contrast to budding yeast, shrinking cMTs in *A. gossypii* showed a very weak or no Bik1 signal at their +tip (Figure 1B, yellow arrowhead). For those six cMTs, we calculated that the cMT depolymerization rate was 0.272 ± 0.075 μm/s (mean ± SD; Figure 2B). This shrinkage rate is also 3 times higher than in budding yeast (*A. gossypii*, 16.3 μm/min vs. *S. cerevisiae*, 4.8 μm/min; Adames *et al*., 2001).

Interestingly, in addition to the bright spot visible at the cMT +tip, lower intensity Bik1 spots were visible along the cMT (Figures 1B and 3A). We hypothesized that those additional Bik1 spots can either be brought to the cMT +tip by a +end directed kinesin motor or moved toward the −end via a −end-directed motor, or alternatively be located at the +tip of a short cMT bundled together with a longer cMT. Figure 2C shows that two Bik1 spots located at the +tip of two cMTs emanating from different SPBs can eventually fuse (fluorescence intensity at t_{30}: spot S1 = 10.8, spot S2 = 7.8; fluorescence intensity at t_{36}: spot S = 17.6). This suggests that a +tip dot of Bik1 could attach to another cMT and move along it to finally form parallel cMT bundles. Bundling of cMT from one SPB or different SPBs may be a way to increase cMT stability. Altogether, the very low frequency of cMT catastrophes, the higher cMT polymerization rate, and the possibility that cMTs form parallel bundles can at least partially explain why cMT grow longer in *A. gossypii* than in budding yeast.

MTs Explore the Cytoplasm and Interact with the Cell Cortex to Induce Nuclear Movements

Interactions between cell cortex and MTs can generate movements of the SPBs and nuclei. Here, we could monitor three different types of dynamic interactions between cMTs

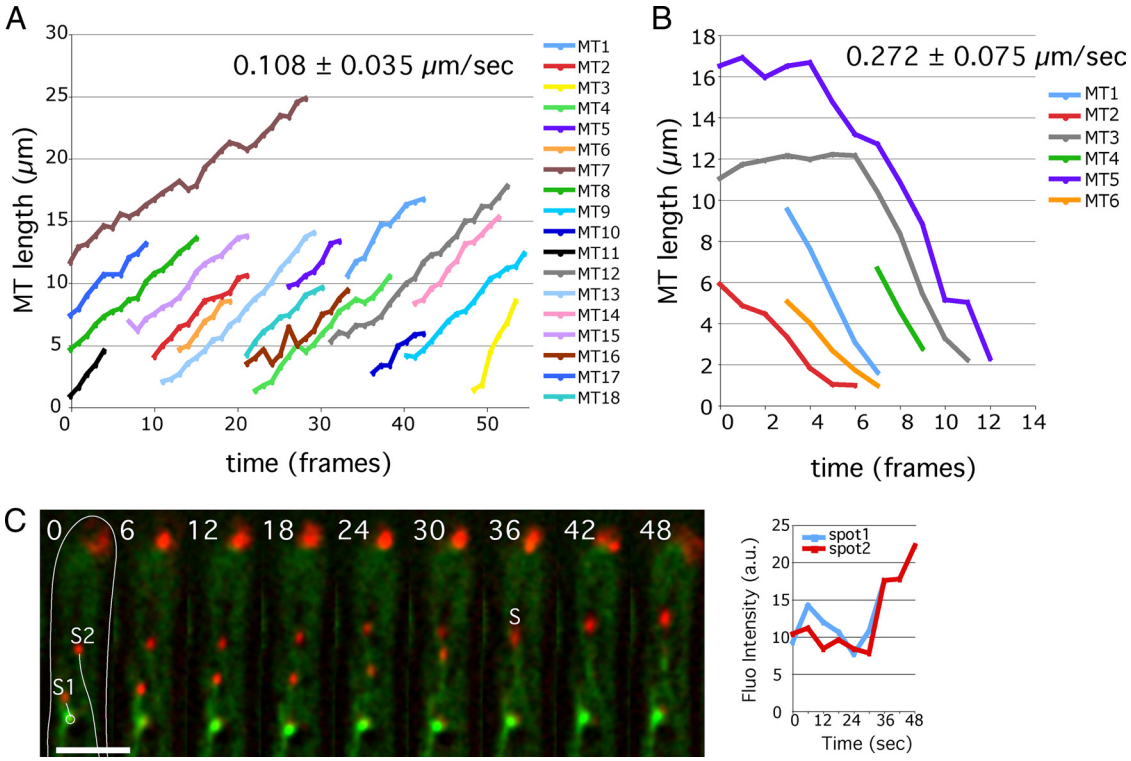

Figure 2. cMT polymerization and depolymerization rates in wild-type *A. gossypii* cells. (A) Quantification of cMT polymerization rate using 1Z plane movies as shown in Figure 1B (using Bik1-Cherry GFP-Tub1 cells). The measured cMTs showed a Bik1 signal at their +end and a strong green dot (GFP-Tub1 at SPBs) at their −end. (B) Quantification of cMT shrinkage rate using 1Z plane movies as shown in Figure 1B. The measured cMTs showed no or a very weak Bik1 signal at their +end and a strong green dot (GFP-Tub1 at SPBs) at their −end. (C) Two Bik1 dots (spots 1 and 2) localizing at the +end of cMTs emanating from different SPBs are merging. Their fluorescence intensities are plotted in arbitrary units. Time is in seconds. Bar, 5 μm.

and the cell cortex. Figure 3A illustrates representative images from three 1Z plane movies made with GFP-Tub1 cells (6-s time intervals). Movie a shows the +end of a cMT interacting with the cortex and while growing up to 5 μm long (t_{36}), the cMT pushed the SPB against the cortex longitudinally (see yellow arrows). In the movie b, the cMT grew against the cortex and pushed the SPB away from it. In contrast to the movie a, the SPB was pushed laterally (see yellow line). In the movie c, one short cMT was rapidly growing to become longer than 5 μm. While growing, the cMT slid along the cell cortex and pulled the SPB in the direction of its +end (t_{36}–t_{60}, see yellow line and white arrows). Very similar to what has been observed in budding yeast, *A. gossypii* cMTs are pushed against, and sweep and slide along the cell cortex, generating SPBs and nuclei movements.

Capture/Shrinkage Mechanisms Are Not Observed in A. gossypii

In yeast, cMTs are directed to the bud neck and the bud tip. After bud emergence, cMTs are growing toward the bud and cMT +tips eventually get captured by the bud neck or the bud tip. After being attached to those specific cortical sites, cMTs are shrinking, therefore pulling nuclei toward the bud tip. In *A. gossypii*, sites where cMT +ends could possibly be captured have not yet been identified. Therefore, we focused our interest on the interactions between MT +ends (Bik1-Cherry signal) and the cell cortex to check whether Bik1 dots eventually stably associate with the cell cortex. As mentioned, this was never the case. While quantifying MT polymerization rate (18 cMTs were analyzed for 23.1 min in total, with 6-s intervals), we could never observe a Bik1 dot localizing at a same site for two consecutive time frames, except for Bik1 localization at hyphal tips. Bik1 dots always moved along the cortex, suggesting that in contrast to budding yeast, cMT +tips were not captured by specific cortical sites. Even though the +ends of cMTs do not stably interact with specific cortical sites, we often see that cMTs maintain lateral contact along their side while sliding forward. Figure 3B shows an example of the sliding forces applied on a SPB by the lateral interaction of a cMT with the cell cortex: the cMT +end touches the cell cortex (t_{36}), grows and curves along it (t_{42}) and then is strongly pulled toward the hyphal tip (t_{42}–t_{54}). However, in contrast to budding yeast, the interactions of the cMT with the hyphal tip do not induce its shrinkage (t_{54}–t_{66}). Even if this is probably indirectly due to its inherent property of being a small surface at the cell end, the cortex of the hyphal tip (and also the septa; see Supplemental Figure 1) could be distinguished from the rest of the cortex because it received a high number of cMT +ends (Figure 1A). Together, by using Bik1 signal as a marker for MT +ends, we concluded that +ends can localize to any place along the hyphal cortex and then actively move along it for relatively long periods (>2 min). No specific cortical MT capture sites seemed to exist in *A. gossypii*; thus, the capture/shrinkage mechanism observed in budding yeast to trigger nuclear movements does not exist in *A. gossypii*.

Bik1 Promotes Microtubule Growth in A. gossypii

The deletion of *BIK1* in budding yeast or of CLIP-170 its mammalian homologue has a drastic effect on MT dynamics.

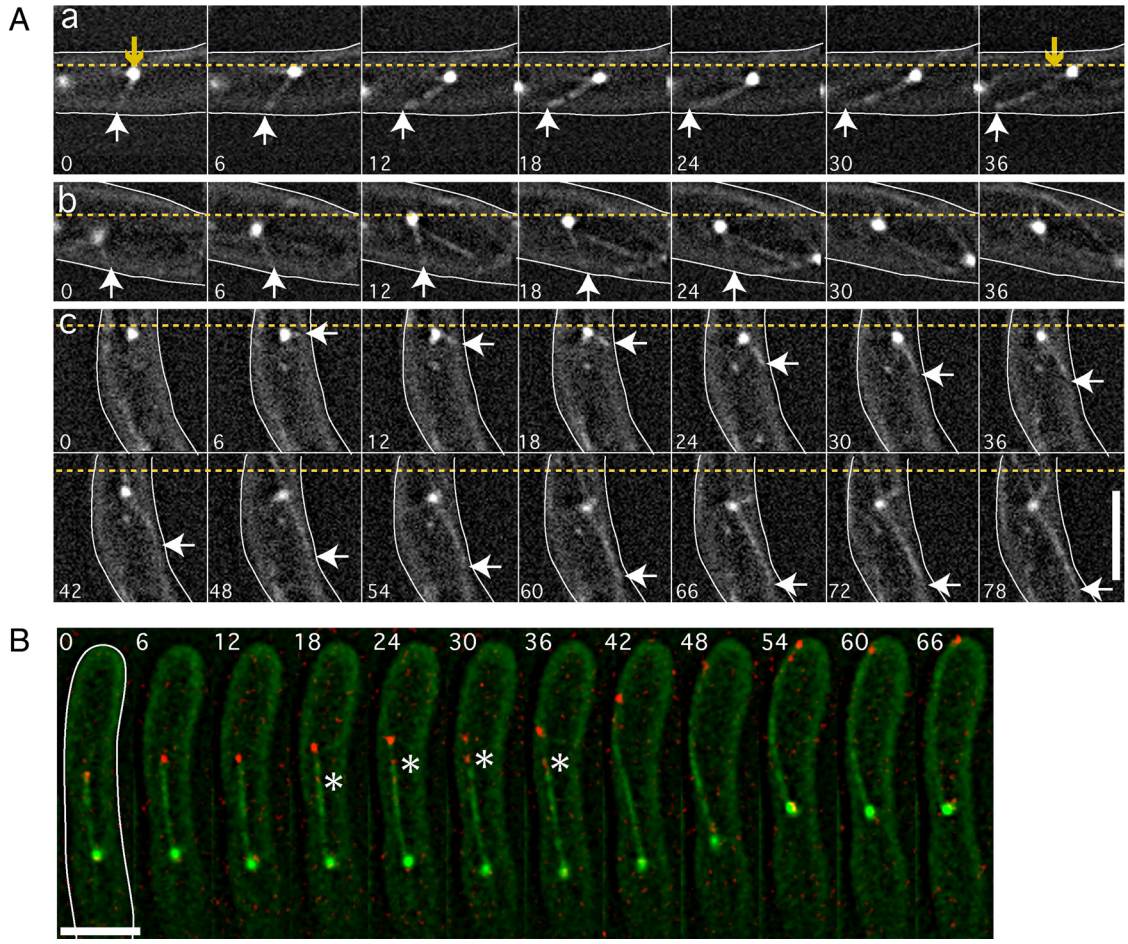

Figure 3. cMT interactions with the cell cortex generate SPB movements in *A. gossypii* cells. (A) Examples of 1Z plane time-lapse movies with GFP-Tub1 cells. a, cMT grows and sweeps the cortex. The SPB does not significantly move laterally but is pushed longitudinally. Yellow arrows represent the position of the SPB at t_0. b, cMT grows and pushes the SPB against the cortex. c, cMT grows and slides along the cortex resulting in a longitudinal SPB movement. a–c, dashed lines represent the uppermost positions of SPBs in the image sequences. The cMT +ends are marked with white arrows. (B) A cMT grows and then slides along the cortex in a GFP-Tub1 Bik1-Cherry hypha (sliding occurs at t_{36}–t_{54}). Asterisk (*) shows a Bik1 dot moving along the cMT. Numbers indicate time in seconds. Bars, 5 μm.

CLIP-170 promotes a high MT rescue frequency and avoids persistent depolymerization when MTs reach the cell periphery (Komarova *et al*., 2002). Deletion of *BIK1* in budding yeast leads to very short cMTs (Berlin *et al*., 1990). ScBik1 stimulates MT dynamics by increasing the rates of growth and shrinkage and by reducing the amount of time cMTs spend in the pause state (Wolyniak *et al*., 2006). In filamentous fungi, deletions of CLIP-170 homologues have milder effects on cMTs. *Aspergilus nidulans* hyphae lacking the CLIP-170 homologue CLIPA still show cMTs extending to hyphal tips even though cMT dynamics is slightly deregulated (Efimov *et al*., 2006).

We deleted the entire open reading frame of the *AgBIK1* gene in wild-type and GFP-TUB1 cells. Anti-α-tubulin immunostaining revealed that short cMTs were still present but the long cMTs observed in wild type were no longer visible in bik1Δ cells (Figure 4A and Table 1). The average cMT length in bik1Δ was 1.67 μm (n = 489; maximum length, 9.5 μm) whereas in wild type, average cMT length was 5.64 μm (n = 335; maximum length, 26.5 μm). To understand how AgBik1 influences cMT dynamics, we performed time-lapse microscopy on bik1Δ GFP-TUB1 hyphae. As mentioned, cMTs were difficult to distinguish in GFP-Tub1 hyphae, but short and long cMTs could be occasionally tracked for >30 s. As shown in Figure 4B, in GFP-TUB1 hyphae, cMTs (white arrows) grew rapidly to reach the cortex, with which they associated. In bik1Δ GFP-TUB1 cells, we could only rarely follow cMTs and only for short periods. Symbols in Figure 4B mark cMTs that either depolymerized (arrowhead) or paused (asterisk) after a short growth phase (arrows). We calculated a cMT polymerization rate of 0.086 ± 0.025 μm/s (mean ± SD; n = 17) in bik1Δ hyphae, which is similar to the polymerization rate of 0.108 ± 0.035 μm/s in WT hyphae (Figure 4C).

Together, these data suggest that in contrast to its homologues in other filamentous fungi, Bik1 is crucial for the control of cMT dynamics in *A. gossypii*. Rather than enhancing the speed of cMT polymerization, AgBik1 seems to promote the processivity of cMT polymerization and stabilize cMTs by avoiding too long pausing time or complete depolymerization.

Long cMTs Enhance the Frequency of MT Sliding Events and Maintain SPBs and Nuclei Close to the Cell Cortex

While measuring cMT dynamics, we noticed that SPBs in bik1Δ mutants were more frequently placed in the center of the hyphae compared with SPBs in wild-type cells. To quantify this, we longitudinally divided hyphae into three equal

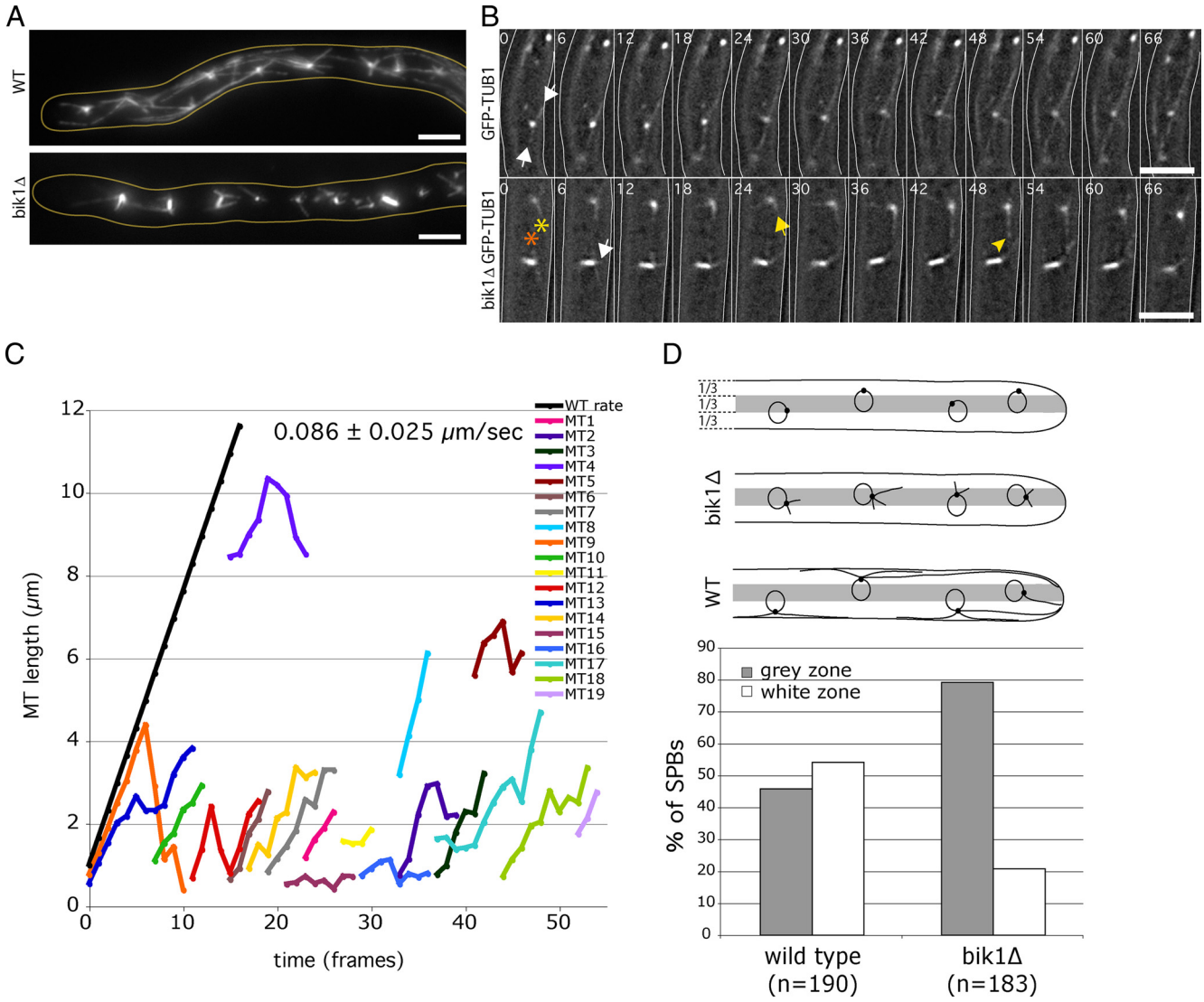

Figure 4. Bik1 promotes cMT growth in *A. gossypii*. (A) Anti-α-tubulin immunostainings in bik1Δ and wild-type cells. Pictures correspond to stacks of 5Z planes with 0.75-μm distance. (B) 1Z plane time-lapse microscopy of bik1Δ and wild-type cells expressing GFP-Tub1. Here, we focused on growth (arrows), pause (*), and shrinkage (arrowheads) of cMTs. (C) Quantification of cMT length in bik1Δ cells. The average WT cMT polymerization rate is shown as reference (black line). (D) Quantification of SPB position in bik1Δ and WT hyphae. SPBs are categorized into two classes: SPB situated in the white cortical zones and SPB situated in the center of the cell (gray zone). Bars, 5 μm.

parts as described in Figure 4D and classified the SPBs in two categories: 1) SPB located in the center of the cell (gray zone) and 2) SPB situated near the cortex (white zones). For these quantifications, we only focused on SPBs belonging to G1 nuclei: 54.2% of SPBs in wild type (GFP-TUB1) are proximal to the cortex, whereas this is the case for only 20.8% of the SPBs in bik1Δ.

As mentioned, in wild-type *A. gossypii* cells long cMTs were sliding along the cell cortex, pulling on SPBs and nuclei and bringing them close to the cortex (see the SPB movement in Figure 3Ac: $t_{36-60\ s}$). These sliding events were not observed in bik1Δ mutants. In budding yeast, cMT sliding depends on the MT motor dynein, in association with its activator dynactin. In Agbik1Δ mutant, sliding does not occur because cMTs are probably too short to be subjected to cortical forces (probably involving dynein). This phenotype also could also suggest that Bik1 by helping to maintain lateral contact of cMTs with the plasma membrane protects them from pausing or depolymerizing as shown in mammalian cells (Komarova *et al.*, 2002). Together, our results suggest that long cMTs are required to maintain SPBs and

Table 1. Measurement of cMT length in WT and mutant *A. gossypii* strains

	Avg. MT length	Max, MT length	No. of MTs
Wild type	5.46	26.5	335
bik1Δ	1.67	9.5	489
kip2Δ	1.33	5.53	438
kip3Δ	6.9	25.6	397

Measurements are in micrometers and were done on anti-α-tubulin immunostaining pictures.

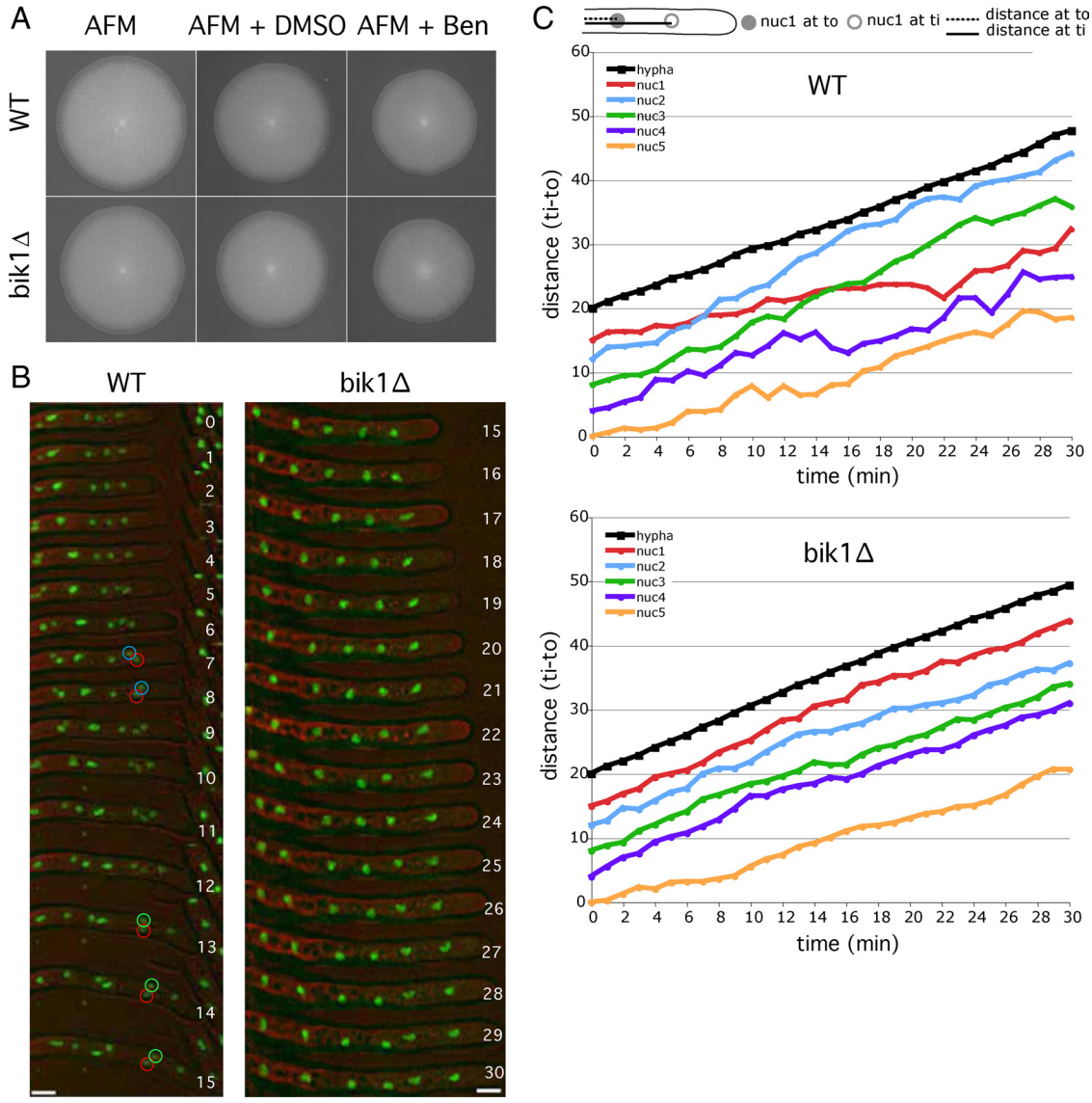

Figure 5. Nuclear distribution and dynamics in wild-type and bik1Δ cells. (A) Radial growth of wild type and bik1Δ mutant after 4 d of incubation on full medium (AFM) at 30°C. Plates containing DMSO are negative controls for benomyl plates. (B) Observation of nuclear dynamics by time-lapse microscopy in wild-type and bik1Δ H4-GFP hyphae. Pictures are overlays of DIC (red) and histone 4-GFP signal. The circles mark bypassing events. Numbers indicate time in min. Bars, 5 μm. (C) Quantification of nuclear oscillation and bypassing in WT and bik1Δ mutant. Distances between a fixed point set at time t_0 and the center of the nuclei were measured at each time point. The first five nuclei shown in B were tracked.

nuclei in proximity to the cell cortex. This may facilitate bypassing events of two nuclei of diameter 2–2.5 μm in a 4- to 4.5-μm large hypha.

Bik1 Is Not Essential for Cell Growth and Only Slightly Affects the Control of Nuclear Spacing

In *A. gossypii*, nuclei divide and migrate toward growing hyphal tips and distribute more or less evenly along hyphae with an average distance of ~5 μm (Gladfelter *et al.*, 2006; Helfer and Gladfelter, 2006; Lang *et al.*, 2010a). Interestingly, even if nuclei actively move back and forth, oscillate, and bypass each other, their overall spacing seems to be regulated. Previous studies have shown that the deletion of the MT motor dynein leads to strong nuclear distribution defects, i.e., all nuclei cluster at the hyphal tips and severely affects cell growth (Alberti-Segui *et al.*, 2001). Because cMTs are not essential for cell growth (Alberti-Segui *et al.*, 2001; Kohli *et al.*, 2008), dyn1Δ phenotypes suggested that cell growth requires a regular nuclear spacing (nuclear clusters could block vesicle transport for example).

To know whether the loss of Bik1 not only affects cMT dynamics and interactions with the cortex but also nuclear distribution, we deleted *BIK1* in a strain in which nuclei were labeled with histone H4-GFP (considered here as a wild-type strain). As shown in Figure 5A, wild-type and bik1Δ strains had similar radial growth after 4 d at 30°C on full medium (AFM). Similar to wild type, bik1Δ spores were able to germinate after 7 h of incubation on AFM at 30°C and displayed a normal cell morphology. The presence of 33 μM of the MT-destabilizing drug benomyl did not affect the growth rate of bik1Δ strains. We observed similar results with bik1Δ GFP-TUB1 strains (data not shown). To measure

Table 2. Quantification of numbers and amplitude of oscillation events in WT and mutant *A. gossypii* strains

	Forward events[a]	Backward events[a]	Bypassing events[a]	Max. forward amplitude[b]	Max. backward amplitude[b]	Avg. growth speed[c]
WT	164	98	9	3.75	3.06	0.75
bik1Δ	76	46	0	2.6	2.6	0.74
kip2Δ	75	32	0	4.14	2.63	0.8
kip3Δ	245	194	28	8.92	7.17	0.77

[a] Total number of events observed during 30 min for 35 nuclei. The five front nuclei of seven different hyphae were followed for 30 min. See examples of movies in Figure 5C). Time interval was 1 min. Definitions for forward and backward are given in the *Results*.

[b] Amplitudes (in micrometers per minute) indicate the maximal distance covered by a nucleus within a 1-min time interval.

[c] This speed is an average of the growth speed of the seven hyphae used for the quantification.

the general spacing of nuclei in wild-type and mutant cells, we classified the distances between two neighboring nuclei (N-N distances) into four categories (Figure 5B). The proportion of 3- to 6-μm N-N distances was twice lower in bik1Δ mutant compared with wild type and almost 20% of the N-N distances were longer than 9 μm in the mutant (4% in WT). Because Bik1 also localized to the central spindle (Supplemental Figure 1), the increased N-N distances in bik1Δ also could result from a lower mitotic index. If anaphases get delayed due to spindle defects, less mitotic events would occur and therefore nuclear density would decrease. Together, our results suggest that the absence of long MTs may only slightly affect the control of nuclear spacing.

Bik1 Is Required for Nuclear Oscillation and Bypassing Events

We have shown above that long cMTs and sliding events are abolished in bik1Δ mutants. Nuclear movements defects in bik1Δ was quantified using 1-min time interval movies with bik1Δ H4-GFP cells. The five nuclei closest to the hyphal tips were tracked for 30 min in seven different wild-type and bik1Δ hyphae (with comparable growth speeds; Table 2 and Figure 5, B and C). Because the overall nuclear migration follows the hyphal growth direction (and the cytoplasmic stream) and because the hyphal growth speed varies for each hypha, we first had to define forward and backward events in wild type to be able to compare it with our mutants. During 1-min time interval, we considered as a forward event a step toward the hyphal tip with twice the speed of the hyphal growth speed. A backward step was stated as a step opposite to the hyphal tip with half the speed of the hyphal growth speed.

The 35 wild-type nuclei performed 164 forward and 98 backward steps in 30 min. In the bik1Δ mutant, only 76 forward and 46 backward events were observed. As illustrated in Figure 5, B and C (also see Table 2), not only the frequency but also the amplitude of bik1Δ nuclear oscillations was strongly reduced compared with wild type. This lack of oscillation was not due to growth speed differences between mutant and wild type (hyphal growth speed for wild type, 0.92 μm/min and for bik1Δ, 0.98 μm/min for examples in Figure 5B; also see Table 2). In addition, no bypassing events were observed for the 35 bik1Δ nuclei during these 30-min movies (9 events in wild type; Table 2).

In conclusion, our results confirmed that long cMTs are required to generate nuclear movements such as bypassing and oscillation. However, it is still unclear whether long cMTs are directly involved in nuclear dynamics by randomly pushing nuclei away from the cell cortex or away from each others, or whether MT motors require long cMTs for effective pulling and directed nuclear movements.

Kinesin Kip2 Is Involved in the Control of cMT Length and Bik1 Localization at cMT +Tips

In budding yeast, Bik1 is targeted to the MT +end by a kinesin-dependent transport mechanism. Bik1 forms a complex with the kinesin Kip2 and both comigrate along individual MTs (Carvalho *et al*., 2004). To determine the mechanism of Bik1 targeting at +end, we tested whether the absence of AgKip2 (42% identity with ScKip2) affected Bik1 localization in *A. gossypii*. Similar to the AgBIK1 deletion, the deletion of AgKIP2 did not affect the hyphal growth rate but led to a severe decrease in cMT length (Supplemental Figure 2 and Table 1). In kip2Δ hyphae, Bik1 accumulation at cMT +ends is strongly reduced or abolished. In contrast, the Bik1-Cherry signal is strongly increased at the SPBs (Figure 6). Therefore, like in budding yeast, AgKip2 has a role in transporting AgBik1 to the +end and probably also in maintaining Bik1 at cMT +ends. In conclusion, the *A. gossypii* kinesin Kip2 is also involved in the control of MT dynamics by delivering Bik1 at MT +tips. Because Kip2 has to bring Bik1 at cMT +end, its velocity along cMTs has to be higher than the cMT polymerization rate (6.5 μm/min). In budding yeast, the Bik1/Kip2 complex moves along the cMTs with an average speed of 6.6 μm/min (Carvalho *et al*., 2004). Finally, consistent with its role in localizing Bik1 at the cMT +ends, we showed that Kip2 is also required for nuclear dynamics. As in bik1Δ mutant, forward and backward events are strongly decreased in kip2Δ cells and bypassing events are abolished (Supplemental Figure 2 and Table 2).

Deletion of the Kinesin Kip3 Increases cMT Length and Frequencies of Oscillation and Bypassing

Recent work has shown that the budding yeast kinesin Kip3 has unique properties. It is both a +end-directed motor and a +end-specific depolymerase that is necessary to regulate the length of MTs attached to the cell cortex and to a lesser extend interpolar MTs (Gardner *et al*., 2008). ScKip3 is observed as speckles that travel toward, and accumulate at, the +ends of growing MTs. However, its accumulation at MT +ends is reduced or absent from depolymerizing +ends (Gupta *et al*., 2006). Varga *et al*. (2006, 2009) proposed a model (the antenna model) in which Kip3 binds randomly along the length of the MT and its high processivity allows it to efficiently target MT +ends. The longer a MT is, the higher the concentration of Kip3 will be at the +end, and the higher the depolymerization rate will be. The dissociation of Kip3 from the +ends is greatly accelerated by incoming Kip3 molecules and is accompanied by removal of one or

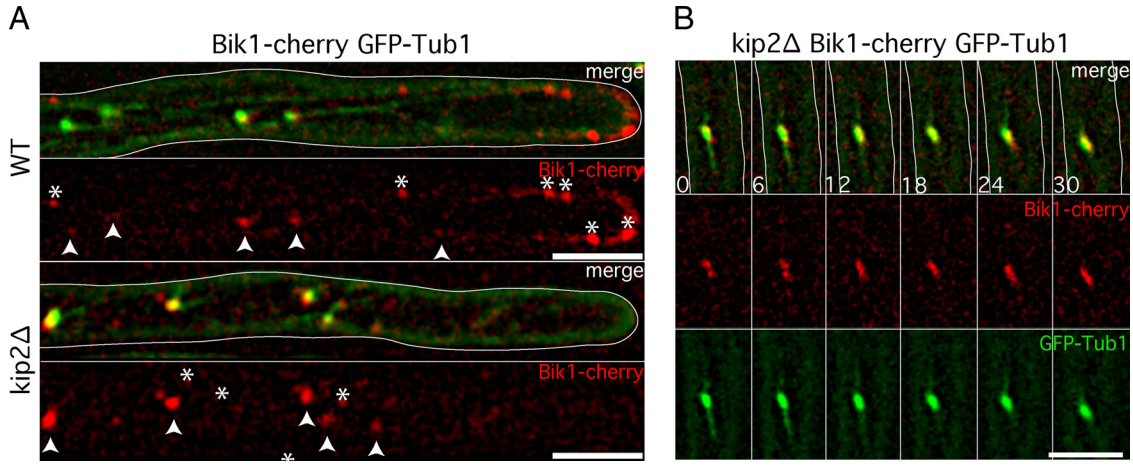

Figure 6. KIP2 deletion affects Bik1 localization at cMT +tips. (A) Bik1 localization in WT (GFP-TUB1) and kip2Δ mutant. In the mutant, Bik1 accumulation is reduced or abolished at cMT +tip (*) and increased at SPB (arrowheads). (B) 1Z plane movie of Bik1-Cherry GFP-Tub1 in kip2Δ background. Numbers indicate time in seconds. Bars, 5 μm.

two tubulin dimers (Varga *et al.*, 2006; Varga *et al.*, 2009). Here, we tested whether AgKip3 (47% identity to ScKip3) has also a role in cMT dynamics and nuclear movements in *A. gossypii*. We deleted the KIP3 gene in hyphae with H4-GFP–labeled nuclei and in hyphae expressing Bik1-Cherry plus GFP-Tub1. The kip3Δ strains grew as well as control strains on full medium and did not show sensitivity or resistance to benomyl (33–132 μM; Figure 7A). However the distances between neighboring nuclei increased clearly in kip3Δ compared with WT cells. The category of N-N distances "over 9 μm" was ~6 times more represented in kip3Δ than in WT (Supplemental Figure 3A). If AgKip3 localizes to the mitotic spindle like its budding yeast homologue, then the increase in N-N distances is probably due to a decrease of the mitotic index in kip3Δ (Miller *et al.*, 1998; Gupta *et al.*, 2006). Overall, this result suggests that the nuclear distance can be increased to a certain extend without affecting the growth rate.

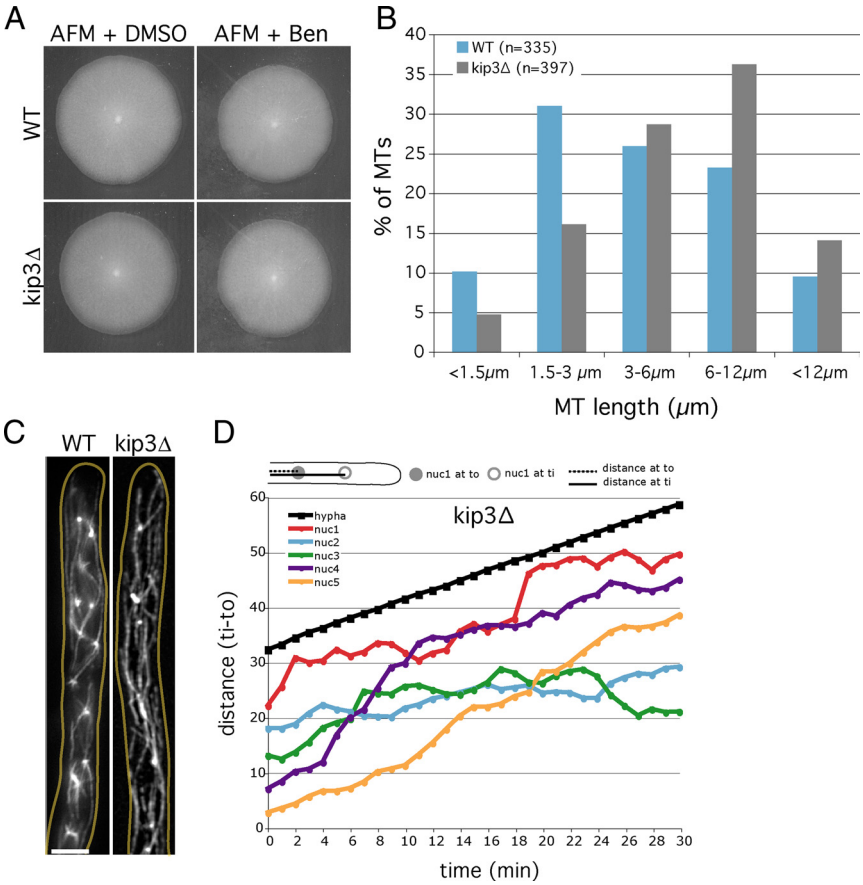

Figure 7. Kinesin Kip3 regulates cMT length and its absence enhances nuclear dynamics in *A. gossypii*. (A) kip3Δ mutant grows like WT. Plates were incubated for 5 d at 30°C on full medium (AFM) containing DMSO (negative control), benomyl at 33 μM, or both. (B) Quantification of cMT length in WT and kip3Δ cells by using anti-Tub1 immunostaining pictures as shown in C. Bar, 5 μm. (D) Quantification of nuclei dynamics in kip3Δ hyphae. Distances between the center of each nucleus and a fixed point were measured for each time point. (E) Quantification of the number of steps the 35 nuclei from Table 2 could consecutively move backward or forward during the 30-min observations. (F) MT polymerization rate in kip3Δ mutant strain. Measurements were made on 6-s interval movies with cells expressing GFP-Tub1 and Bik1-cherry fusions (only 1Z plane was observed). cMTs were measured from their −end (SPB observed with GFP-Tub1) until their +tip (Bik1-cherry signal). Due to increased cMT length in kip3Δ strain, SPBs and +tips were often in different focal planes. Asterisk (*) corresponds to the actual length of the cMTs (SPB to +tip), whereas the other MTs have an underestimated size (visible part of cMT to +tip). 1 time frame corresponds to 6 s. The average WT cMT polymerization rate is shown as reference (black line).

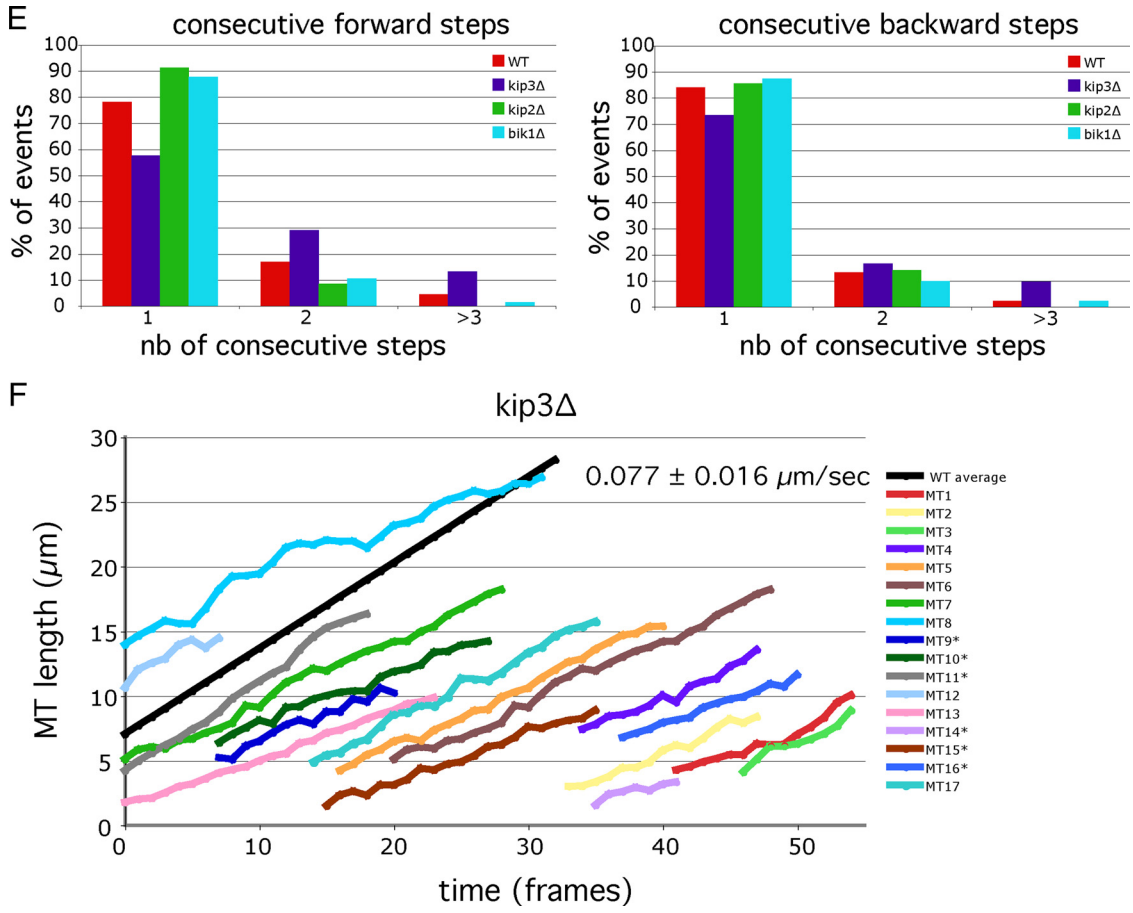

Figure 7. *Continued.*

Using anti-tubulin staining, we also noticed that cMTs were longer in kip3Δ, suggesting that AgKip3 has a role in shortening or destabilizing cMTs (Figure 7, B and C, and Table 1; average MT length in WT, 5.46 μm, 32.8% of cMTs >6 μm; in kip3Δ, 6.90 μm, 50.4% of cMTs >6 μm). As described previously for WT and the kip2Δ mutant, we quantified the position of SPBs relative to the hyphal cortex in the kip3Δ mutant and found that 58.7% of the SPBs of kip3Δ cells were situated near the cell cortex. This is similar to WT (54.2% of SPBs near the cortex; Figure 4D) and consistent with our previous conclusion that long cMTs are required to maintain SPBs in proximity to the cortex. The most striking phenotype was the increase in nuclear bypassing frequencies and oscillation amplitudes in kip3Δ hyphae (Figure 7, D and E, and Table 2). As described above for the bik1Δ mutant, we quantified the nuclear movements of 35 nuclei for 30 min and observed 3 times more bypassing events in the kip3Δ mutant than in WT. Forward and backward events were, respectively, increased 1.5 and 2 times compared with WT, and the rate of consecutive forward and backward movements also increased (consecutive forward steps >1 in WT, 21.7%; in kip3Δ, 42.4%; consecutive backward steps >1 in WT, 15.8%; in kip3Δ, 21.7%). In addition, the distance between the first nucleus and the hyphal tip in kip3Δ cells compared with WT is not significantly changed, similarly as in bik1Δ and kip2Δ hyphae which form cMTs shorter than WT (Supplemental Figure 3B). Thus, the observed size differences in cMTs in these three mutants still allow to keep contact of the leading nucleus with the growing tip.

Together, these results strongly suggest that AgKip3 is a MT depolymerase like its budding yeast homologue and that the frequency and amplitude of nuclear movements in *A. gossypii* are cMT dependent.

Oscillation and Bypassing Events Are Mainly Due to Pulling Forces Applied on cMTs and Not Pushing Forces

To test how cMT dynamics was changed in kip3Δ, we measured cMT polymerization rate in the mutant labeled with Bik1-Cherry and GFP-Tub1. Interestingly, we observed that the cMT polymerization rate in kip3Δ was slightly reduced compared with WT (kip3Δ, 0.077 ± 0.016 μm/s; WT, 0.108 ± 0.035 μm/s; Figure 7F). Because the maximal oscillation amplitude measured for kip3Δ cells was 8.92 μm/min, we could conclude that this event was not caused by the push of a fast-growing cMT against the cell cortex (average cMT growth rate of kip3Δ, 4.62 μm/min; minimum, 2.90 and maximum, 6.54 μm/min). Then, these fast moving nuclei in kip3Δ cells were most probably resulting from increased pulling forces applied on cMTs. We propose therefore a model in which nuclei bypassing and oscillatory movements are mainly dependent on a MT motor exerting pulling forces on SPBs via their cMTs. This motor (probably dynein) would be associated to the cell cortex because cMT sliding along the cortex are often visible in *A. gossypii*. In this model, the loading of the dynein motor on cMTs could be proportional to the length of the cMTs. The higher dynein concentration is on cMTs the faster nuclei can be pulled and oscillate. Alternatively, increasing the length of cMTs also could increase their chance of interacting with the cell cortex and

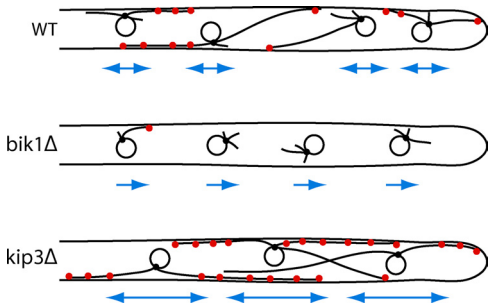

Figure 8. Amplitudes of nuclear oscillation and bypassing events depend on cMT length. Long cMTs in Agkip3Δ have longer lateral interactions with the cell cortex compared with WT and are subjected to more pulling forces (most probably dynein dependent forces, red dots). The shorter cMTs in Agbik1Δ (and also in Agkip2Δ; not shown) rarely have lateral interactions with the cortex. For reasons of clarity, numbers of nuclei, cMTs, and hyphal tip-accumulated cMT +ends are underrepresented in the depicted hyphae.

with some specific proteins required to stimulate the pulling activity of the dynein motor (Figure 8). The clustering of nuclei in hyphal tips, reported previously for an Agdyn1Δ strain seems to contradict the model of this figure (Alberti-Segui *et al*., 2001). It is very likely that the nuclear clustering which is already observed in tips of *A. gossypii* germlings is caused by the extremely long cMTs, which form in the absence of dynein, thus pushing the nuclei toward the tips as documented in Alberti-Segui *et al*. (2001).

DISCUSSION

The two major goals of this work were to understand how cMT dynamics participates to nuclear movements and to investigate how cMT dynamics is controlled in the multinucleated *A. gossypii* cells. We have characterized the dynamic intracellular distribution of Bik1. Our results revealed a Kip2-dependent mechanism for targeting Bik1 to cMT +ends and showed that in contrast to its budding yeast homologue, AgBik1 dissociates from shrinking cMTs. We showed that the kinesin Kip3 contributes to cMT depolymerization and that cMT shrinkage/catastrophe are seldom events in *A. gossypii*. Finally, our findings showed that the overall length of cMTs is a more important factor for the control of nuclear movements than cMT dynamicity.

Nuclear Movements in A. gossypii Are Not Controlled by cMT Dynamic Instability

MT dynamics is determined by four parameters: the speed of MT growth, the speed of MT shrinkage, the frequency of catastrophe (transitions from growth to shrinkage phase), and the frequency of rescues (transitions from shrinkage to growth phase). MTs can also be in a pause state (Desai and Mitchison, 1997; Akhmanova and Steinmetz, 2008; van der Vaart *et al*., 2009). In *A. gossypii*, we first hypothesized that like in other organisms, dynamic instability would occur to allow cMTs to probe the cell for specific cortical sites. In budding yeast, cMTs ensure that the mitotic spindle is properly positioned relative to the cleavage apparatus. The septins are required to form a cMT-capture site at the bud neck cortex, and septin-dependent kinases are suggested to induce cMT catastrophe and pulling forces on the spindle, which then move toward the bud neck (Kusch *et al*., 2002). The incipient bud site is another important site for cMTs capture followed by shrinkage (Adames and Cooper, 2000; Lee *et al*., 2000). The Bim1, Bud6, Bni1, and Kar9 proteins involved in the capture/shrinkage mechanism in budding yeast are all present in *A. gossypii*. However, our preliminary experiments have shown that the absence of Kar9 and Bim1 proteins does not significantly affect nuclear distribution (Grava, unpublished data). This supports our interpretations that in *A. gossypii*, cMT +ends are not captured by specific cortical sites. However we cannot exclude rare events similar to capture/shrinkage observed in *S. cerevisiae*. Here, we also show that cMTs do not show alternated phases of growth and shrinkage. cMT +ends are therefore not inducing nuclear movements via depolymerization. In *A. gossypii*, it is possible that the mechanism of specific cMT capture and positioning of nuclei has not been developed or has been lost during evolution because cell separation does not occur and hyphal compartments can share eight to nine nuclei. The strong nuclei and SPBs oscillations observed in hyphae are therefore probably due to MT motor-dependent sliding of cMTs along the cell cortex.

Nuclear Movements in A. gossypii Require Prolonged MT Growth Phases

Our time lapse microscopy of GFP-labeled MTs has provided key insight into the regulation of nuclear movements in *A. gossypii*. On one hand, when a short cMT grows against the cell cortex, it pushes the SPB and nucleus away from the cortex and induces micromovements of SPB and nuclei. On the other hand, when a cMT grows for a longer period, prolonged lateral interaction of this cMT with the cell cortex induces its sliding along the cell cortex. These sliding events produce much more efficient nuclear movements (toward the site of cortical attachment) than pushing events. The idea that cMT length is an essential factor in the control of nuclear movements is also supported by 1) the loss of oscillation and bypassing events in the bik1Δ and kip2Δ mutants, in which cMTs are much shorter than in wild-type cells; and 2) the higher frequency and amplitude of nuclear movements in the kip3Δ mutant, in which cMTs are longer than in WT. In budding yeast, sliding of cMTs along the cell cortex depends on a dynein-driven pulling mechanism. The "off-loading model" proposes that dynein first accumulates at cMT +tips, then gets anchored to the cortex, and finally its −end stepping behavior moves the MT past the fixed motor (Lee *et al*., 2003; Sheeman *et al*., 2003).

If dynein is responsible for cMT pulling in *A. gossypii*, the nuclear oscillation differences between kip2Δ/bik1Δ and kip3Δ mutants could be explained in the following way: the pulling force applied on long cMTs is increased due to a higher concentration of dynein on MTs (or specifically at their +ends). It is not known exactly how dynein gets loaded on budding yeast MTs. However, it has been shown that the accumulation of dynein at +ends requires Bik1 and Kip2. If dynein binds at a random position on MTs and then moves toward the +end via Kip2/Bik1, the longer a cMT is, the higher the concentration of Kip2/Bik1 and/or dynein could be on cMTs. Alternatively, the pulling force applied on longer cMTs could be increased due to longer lateral interactions of cMTs with the cell cortex. If the MT motor responsible for cMT sliding in *A. gossypii* is associated with the plasma membrane, increasing cMT length will increase the probability a cMT can interact with such a MT motor and will also increase the number of motors interacting with the cMT (Figure 8).

Considering that an SPB can nucleate up to six cMTs, another concern for the future will be to understand how each SPB can coordinate the forces applied on cMTs. Non-

oscillatory movements could be either the results of equal forces applied on cMTs of the same length but pulling in opposite directions or could be due to the lack of interactions between cMTs and the cell cortex. In contrast, bypassing and oscillations could occur when the forces applied on SPBs are unbalanced either due to strong differences in cMT length or to pulling of several cMTs in one direction.

Differences in cMT Dynamics between Budding Yeast and A. gossypii

A. gossypii hyphae can grow up to 3 μm/min. As shown with Bik1-Cherry, many MTs +ends emanating from at least the four to five most apical SPB and nuclei can reach the tips of the growing hyphae. This suggests that in *A. gossypii* cMT cytoskeleton has to adapt to these fast-growing cells and need to increase cMT growth speed consequently. Our results show clear differences in cMT dynamics between budding yeast and *A. gossypii*. Growth rate is indeed increased in *A. gossypii* and can partially account for differences in cMT length between the two organisms. However, the cMT length differences between yeast and *A. gossypii* probably not only depend on speed of polymerization or depolymerization but also on the length of the polymerization and depolymerization phases (or processivity). Interestingly, the frequency of cMT shrinkage seems to be very low in *A. gossypii*. These observations especially concern the cMTs longer than 2 μm. Because of the high number of cMTs emanating from a SPB (up to 6 cMTs) and the strong fluorescence background around it, it is difficult to follow shrinkage or pause of cMTs shorter than 2 μm. But why is MT polymerization rate 3 times higher in *A. gossypii* than in budding yeast and why are catastrophes rare events? Several recent reviews compiled the current mechanistic models for MT dynamic instability and emphasized its complexity (Hammond *et al*., 2008; Howard and Hyman, 2009; Slep, 2010). Dynamic instability depends on the capacity of α/β-tubulins to self-assemble and to hydrolyze GTP at MT +tips. In budding yeast, α-tubulin is encoded by two genes, TUB1 and TUB3, whereas it is only encoded by one gene in *A. gossypii* (AgTUB1). ScTub3 represents ~10% of α-tubulin in the cell and contribute to the intrinsic stability of yeast MTs in vitro by decreasing the rate of depolymerization and the frequency of catastrophe (Bode *et al*., 2003). On the 39 residues that are different between ScTub1 and ScTub3, 26 residues of AgTub1 are identical to ScTub1, eight are identical to ScTub3, and five are specific to the *A. gossypii* protein. These changes could result in conformational changes in the tubulin dimers, modify their GTPase activity, or affect interactions with MT-associated proteins and could therefore explain the differences between *A. gossypii* and budding yeast cMT dynamics.

Bik1, the Kinesin Kip2 and cMT Dynamics

Previous work based on anti-tubulin staining techniques has proposed that two categories of cMTs can be distinguished in *A. gossypii*: short cMTs interacting with the cell cortex via their +ends (<5 μm long) and >5-μm-long cMTs making lateral contact with the cell cortex. These short and long cMTs also were proposed to emanate from SPBs with different orientations: perpendicular and tangential to SPB layers respectively (Lang *et al*., 2010a,b). Our in vivo studies of cMT dynamics using GFP-Tubulin1 and Bik1-Cherry markers showed that distinction between short and long cMTs does not really exists because short cMTs can rapidly grow up to 25 μm. The presence of short and long cMTs at one specific time point of the GFP-Tub1 movies [or anti-tubulin immunostaining or electron microscopy pictures in Lang *et al*. (2010a)] results from cMT dynamics. However, cMTs could be distinguished according their ability to accumulate Bik1 at their +tips. We observed very short cMTs (<2 μm long) that lack Bik1 at their +ends and seem to move more rapidly out of the focal plane than the long cortical cMTs or quickly depolymerize (shrink within a 6-s time frame). Their +tips are not necessarily interacting with the cell cortex. Moreover, even though shrinking cMTs (>2 μm long) are rarely observed, they never accumulate Bik1 at their +ends. Only the cMTs showing a Bik1-Cherry signal at their +tips rapidly grow longer than 5 μm and can be followed for up to 2 min. Interestingly, they are in constant growing phase, their +tips often grow along the cell cortex and do not show any dynamic instability. This results revealed a clear difference with the budding yeast Bik1 that binds both polymerizing and depolymerizing cMTs (Carvalho *et al*., 2004). The mammalian functional homologue of Bik1, CLIP-170 preferentially associates with growing rather than depolymerizing MTs. CLIP-170 treadmills along these MT +ends to maintain the association with the extending MT tip. Those interactions seem to stabilize MTs by connecting them to the cell cortex (Perez *et al*., 1999; Slep, 2010). Similar to budding yeast, our data strongly support the idea that AgBik1 does not treadmill with the +tips but is targeted to cMT +ends by the kinesin Kip2. Because Kip2 is essential to bring Bik1 at cMT +tips, it will be interesting to characterize Kip2 localization in *A. gossypii* and see whether the +tip localization of Kip2 is also reduced or absent on shrinking cMTs. Investigating the mechanisms which control Bik1 and Kip2 localization at MT +ends in budding yeast and in *A. gossypii* could help in the future to understand the differences in cMT length between the two organisms.

CONCLUSIONS

The multinucleate growth mode of *A. gossypii* has resulted in a unique control of cytoplasmic MT dynamics. The near to normal growth of hyphae in the absence of cMTs make *A. gossypii* an attractive model organism to study biological effects of mutants with altered cMT dynamics. Through our analysis of MT +tips behavior and cMT–cell cortex interactions, we elucidated the necessity of *A. gossypii* to produce very long MTs for nuclear migration to compensate the lack of MT capture/shrinkage mechanisms important to position nuclei in other organisms. Our new data demonstrate evolutionary diversity of the control of MT dynamics and of the role of MT +tips proteins and kinesins between two closely related organisms, *S. cerevisiae* and *A. gossypii*.

ACKNOWLEDGMENTS

We thank Shanon Seger, Eloïse Kremer, and Clara Metz for help in strain construction. We acknowledge the advice and suggestions of Sue Jaspersen and Claudia Lang. We also thank Christine Alberti-Segui for providing unpublished data. This work was supported by the Swiss National Science Foundation grant 3100A0-112688 (to P. P.).

REFERENCES

Adames, N. R., and Cooper, J. A. (2000). Microtubule interactions with the cell cortex causing nuclear movements in *Saccharomyces cerevisiae*. J. Cell Biol. *149*, 863–874.

Ahringer, J. (2003). Control of cell polarity and mitotic spindle positioning in animal cells. Curr. Opin. Cell Biol. *15*, 73–81.

Akhmanova, A., and Steinmetz, M. O. (2008). Tracking the ends: a dynamic protein network controls the fate of microtubule tips. Nat. Rev. Mol. Cell Biol. *9*, 309–322.

Alberti-Segui, C., Dietrich, F., Altmann-Johl, R., Hoepfner, D., and Philippsen, P. (2001). Cytoplasmic dynein is required to oppose the force that moves nuclei towards the hyphal tip in the filamentous ascomycete *Ashbya gossypii*. J. Cell Sci. *114*, 975–986.

Ayad-Durieux, Y., Knechtle, P., Goff, S., Dietrich, F., and Philippsen, P. (2000). A PAK-like protein kinase is required for maturation of young hyphae and septation in the filamentous ascomycete *Ashbya gossypii*. J. Cell Sci. *113*, 4563–4575.

Berlin, V., Styles, C. A., and Fink, G. R. (1990). BIK1, a protein required for microtubule function during mating and mitosis in *Saccharomyces cerevisiae*, colocalizes with tubulin. J. Cell Biol. *111*, 2573–2586.

Bode, C. J., Gupta, M. L., Suprenant, K. A., and Himes, R. H. (2003). The two alpha-tubulin isotypes in budding yeast have opposing effects on microtubule dynamics in vitro. EMBO Rep. *4*, 94–99.

Brunner, D., and Nurse, P. (2000). CLIP170-like tip1p spatially organizes microtubular dynamics in fission yeast. Cell *102*, 695–704.

Carvalho, P., Gupta, M. L., Jr., Hoyt, M. A., and Pellman, D. (2004). Cell cycle control of kinesin-mediated transport of Bik1 (CLIP-170) regulates microtubule stability and dynein activation. Dev. Cell *6*, 815–829.

Carvalho, P., Tirnauer, J. S., and Pellman, D. (2003). Surfing on microtubule ends. Trends Cell Biol. *13*, 229–237.

Caudron, F., Andrieux, A., Job, D., and Boscheron, C. (2008). A new role for kinesin-directed transport of Bik1p (CLIP-170) in *Saccharomyces cerevisiae*. J. Cell Sci. *121*, 1506–1513.

Coquelle, F. M., *et al*. (2002). LIS1, CLIP-170's key to the dynein/dynactin pathway. Mol. Cell. Biol. *22*, 3089–3102.

Desai, A., and Mitchison, T. J. (1997). Microtubule polymerization dynamics. Annu. Rev. Cell. Dev. Biol. *13*, 83–117.

DeZwaan, T. M., Ellingson, E., Pellman, D., and Roof, D. M. (1997). Kinesin-related KIP3 of *Saccharomyces cerevisiae* is required for a distinct step in nuclear migration. J. Cell Biol. *138*, 1023–1040.

Dietrich, F. S., *et al*. (2004). The *Ashbya gossypii* genome as a tool for mapping the ancient *Saccharomyces cerevisiae* genome. Science *304*, 304–307.

Efimov, V. P., Zhang, J., and Xiang, X. (2006). CLIP-170 homologue and NUDE play overlapping roles in NUDF localization in *Aspergillus nidulans*. Mol. Biol. Cell *17*, 2021–2034.

Galjart, N., and Perez, F. (2003). A plus-end raft to control microtubule dynamics and function. Curr. Opin. Cell Biol. *15*, 48–53.

Gardner, M. K., *et al*. (2008). Chromosome congression by kinesin-5 motor-mediated disassembly of longer kinetochore microtubules. Cell *135*, 894–906.

Gladfelter, A., and Berman, J. (2009). Dancing genomes: fungal nuclear positioning. Nat. Rev. Microbiol. *7*, 875–886.

Gladfelter, A. S., Hungerbuehler, A. K., and Philippsen, P. (2006). Asynchronous nuclear division cycles in multinucleated cells. J. Cell Biol. *172*, 347–362.

Gupta, M. L., Jr., Carvalho, P., Roof, D. M., and Pellman, D. (2006). Plus end-specific depolymerase activity of Kip3, a kinesin-8 protein, explains its role in positioning the yeast mitotic spindle. Nat. Cell Biol. *8*, 913–923.

Hammond, J. W., Cai, D., and Verhey, K. J. (2008). Tubulin modifications and their cellular functions. Curr. Opin. Cell Biol. *20*, 71–76.

Helfer, H., and Gladfelter, A. S. (2006). AgSwe1p regulates mitosis in response to morphogenesis and nutrients in multinucleated *Ashbya gossypii* cells. Mol. Biol. Cell *17*, 4494–4512.

Howard, J., and Hyman, A. A. (2009). Growth, fluctuation and switching at microtubule plus ends. Nat. Rev. Mol. Cell Biol. *10*, 569–574.

Kaufmann, A. (2009). A plasmid collection for PCR-based gene targeting in the filamentous ascomycete *Ashbya gossypii*. Fungal Genet. Biol. *46*, 595–603.

Kohli, M., Galati, V., Boudier, K., Roberson, R. W., and Philippsen, P. (2008). Growth-speed-correlated localization of exocyst and polarisome components in growth zones of *Ashbya gossypii* hyphal tips. J. Cell Sci. *121*, 3878–3889.

Komarova, Y. A., Akhmanova, A. S., Kojima, S., Galjart, N., and Borisy, G. G. (2002). Cytoplasmic linker proteins promote microtubule rescue in vivo. J. Cell Biol. *159*, 589–599.

Kusch, J., Meyer, A., Snyder, M. P., and Barral, Y. (2002). Microtubule capture by the cleavage apparatus is required for proper spindle positioning in yeast. Genes Dev. *16*, 1627–1639.

Lang, C., Grava, S., Finlayson, M., Trimble, R., Philippsen, P., and Jaspersen, S. L. (2010b). Structural mutants of the spindle pole body cause distinct alteration of cytoplasmic microtubules and nuclear dynamics in multinucleated hyphae. Mol. Biol. Cell *21*, 753–766.

Lang, C., Grava, S., van den Hoorn, T., Trimble, R., Philippsen, P., and Jaspersen, S. L. (2010a). Mobility, microtubule nucleation and structure of microtubule-organizing centers in multinucleated hyphae of *Ashbya gossypii*. Mol. Biol. Cell *21*, 18–28.

Lee, L., Klee, S. K., Evangelista, M., Boone, C., and Pellman, D. (1999). Control of mitotic spindle position by the *Saccharomyces cerevisiae* formin Bni1p. J. Cell Biol. *144*, 947–961.

Lee, L., Tirnauer, J. S., Li, J., Schuyler, S. C., Liu, J. Y., and Pellman, D. (2000). Positioning of the mitotic spindle by a cortical-microtubule capture mechanism. Science *287*, 2260–2262.

Lee, W. L., Oberle, J. R., and Cooper, J. A. (2003). The role of the lissencephaly protein Pac1 during nuclear migration in budding yeast. J. Cell Biol. *160*, 355–364.

Lin, H., de Carvalho, P., Kho, D., Tai, C. Y., Pierre, P., Fink, G. R., and Pellman, D. (2001). Polyploids require Bik1 for kinetochore-microtubule attachment. J. Cell Biol. *155*, 1173–1184.

Miller, R. K., Heller, K. K., Frisen, L., Wallack, D. L., Loayza, D., Gammie, A. E., and Rose, M. D. (1998). The kinesin-related proteins, Kip2p and Kip3p, function differently in nuclear migration in yeast. Mol. Biol. Cell *9*, 2051–2068.

Moore, A., and Wordeman, L. (2004). The mechanism, function and regulation of depolymerizing kinesins during mitosis. Trends Cell Biol. *14*, 537–546.

Perez, F., Diamantopoulos, G. S., Stalder, R., and Kreis, T. E. (1999). CLIP-170 highlights growing microtubule ends in vivo. Cell *96*, 517–527.

Shaw, S. L., Yeh, E., Maddox, P., Salmon, E. D., and Bloom, K. (1997). Astral microtubule dynamics in yeast: a microtubule-based searching mechanism for spindle orientation and nuclear migration into the bud. J. Cell Biol. *139*, 985–994.

Sheeman, B., Carvalho, P., Sagot, I., Geiser, J., Kho, D., Hoyt, M. A., and Pellman, D. (2003). Determinants of *S. cerevisiae* dynein localization and activation: implications for the mechanism of spindle positioning. Curr. Biol. *13*, 364–372.

Slep, K. C. (2010). Structural and mechanistic insights into microtubule end-binding proteins. Curr. Opin. Cell Biol. *22*, 88–95.

Sproul, L. R., Anderson, D. J., Mackey, A. T., Saunders, W. S., and Gilbert, S. P. (2005). Cik1 targets the minus-end kinesin depolymerase kar3 to microtubule plus ends. Curr. Biol. *15*, 1420–1427.

Tirnauer, J. S., O'Toole, E., Berrueta, L., Bierer, B. E., and Pellman, D. (1999). Yeast Bim1p promotes the G1-specific dynamics of microtubules. J. Cell Biol. *145*, 993–1007.

van der Vaart, B., Akhmanova, A., and Straube, A. (2009). Regulation of microtubule dynamic instability. Biochem. Soc. Trans. *37*, 1007–1013.

Varga, V., Helenius, J., Tanaka, K., Hyman, A. A., Tanaka, T. U., and Howard, J. (2006). Yeast kinesin-8 depolymerizes microtubules in a length-dependent manner. Nat. Cell Biol. *8*, 957–962.

Varga, V., Leduc, C., Bormuth, V., Diez, S., and Howard, J. (2009). Kinesin-8 motors act cooperatively to mediate length-dependent microtubule depolymerization. Cell *138*, 1174–1183.

Wendland, J., Ayad-Durieux, Y., Knechtle, P., Rebischung, C., and Philippsen, P. (2000). PCR-based gene targeting in the filamentous fungus *Ashbya gossypii*. Gene *242*, 381–391.

Wendland, J., and Walther, A. (2005). *Ashbya gossypii*: a model for fungal developmental biology. Nat. Rev. Microbiol. *3*, 421–429.

Wolyniak, M. J., Blake-Hodek, K., Kosco, K., Hwang, E., You, L., and Huffaker, T. C. (2006). The regulation of microtubule dynamics in *Saccharomyces cerevisiae* by three interacting plus-end tracking proteins. Mol. Biol. Cell *17*, 2789–2798.